Adaptive Carrier Recovery Systems for Digital Data Communications Receivers

ROBERT L. CUPO, MEMBER, IEEE, AND RICHARD D. GITLIN, FELLOW, IEEE

Abstract—Adaptive or predictive, carrier recovery systems are essential in high-performance quadrature amplitude modulated (QAM) data communications systems to correct for phase jitter and frequency offset. In this study we present analytical and experimental results for two structures that implement a predictive carrier recovery system. These systems, which adapt their structure to match the spectral properties of the impairments, avoid the conflict between a wide bandwidth (to track fast jitter) and a narrow bandwidth (to minimize output noise) inherent in most carrier recovery loops. Such a system increases the likelihood that very bandwidth-efficient modems (e.g., 7 bits/s/Hz for 19.2 Kbits/s voiceband modem applications) can provide reliable transmission in the presence of severe phase jitter and frequency offset. In particular, the predictive carrier recovery systems can track sinusoidal jitter present at more than one frequency, as well as generalized time-varying phase jitter processes.

We consider both finite impulse response (FIR) and infinite impulse response (IIR) adaptive phase tracking systems. We overcome prior limitations on adaptive IIR filters by designing a structure that is guaranteed to be stable and to possess only a global minimum as the filter coefficients converge to their desired values. These adaptive structures represent a significant advance over the performance attainable by conventional carrier-tracking loops.

I. Introduction

In quadrature amplitude modulated (QAM) digital data communication systems, errors associated with extreme amounts of phase jitter are a potential impediment to achieving the desired system performance. This study focuses on several novel adaptive carrier recovery systems which mitigate the effect of this impairment. The techniques proposed in this paper are substantially more powerful than the nonadaptive, data-directed techniques used in conventional data receivers [1] which are a compromise between wide-band systems for jitter tracking and narrow-band systems for noise rejection. Incorporation of these novel adaptive carrier recovery systems may be necessary to achieve reliable operation of high-performance ($\sim$6–8 bits/s/Hz) data communications systems. The techniques described in this paper may also be used in systems employing trellis coded modulation. Furthermore, these adaptive structures can track jitter appearing at more than one frequency, and in the absence of jitter, the adaptive loop will strive to minimize the noise appearing at the loop output.

In Section II, we review the well-known form of compensation, the data-directed second-order phase locked loop. The characteristics of an adaptive FIR filter are derived in Section III. Section IV introduces an adaptive IIR filter structure, which is compared to the adaptive FIR structure in Section V. Our conclusions are given in Section VI.

We begin with a model and a description of carrier error for QAM systems. First, it is assumed that transmission is ideal, except for the phase errors associated with the carrier at the output of the adaptive equalizer, in the QAM data communications receiver shown in Fig. 1. Referring to Fig. 1,

$$x(n) = a(n)e^{j(\omega_c nT + \theta(n))} + v(n) \tag{1}$$

where

$x(n)$	is the output of a passband equalizer
$a(n) = a_r(n) + ja_i(n)$	is the nth transmitted symbol (a discrete-valued complex number) representing the in-phase $a_r(n)$ and quadrature $a_i(n)$ data
ω_c	is the known transmitted carrier frequency
T	is the symbol period
$\theta(n)$	is the uncompensated carrier phase at the receiver input [$\hat{\theta}(n)$ will be used to denote an estimate of $\theta(n)$] and
$v(n)$	is additive white Gaussian noise.

The carrier error $\theta(n)$ will generally have three components: phase jitter, frequency offset, and phase offset. The phase jitter is typically modeled as sinusoidal, and is mainly due to power-line harmonics and ringing voltages. Frequency offset is the shift given to the signal as it propagates through the channel carrier system. Phase offset is simply a constant phase difference between transmit and receive carriers. These comments lead to the following mathematical model for the carrier phase at the (symbol-rate) samplings instants:

$$\theta(n) = \omega_o nT + \sum_{j=0}^{J} A_j \sin \omega_j T + \theta_0 \tag{2}$$

where

ω_o is the amount of frequency offset
A_j is the amplitude of the sinusoidal phase jitter at

Manuscript received April 25, 1988; revised December 3, 1988.
R. L. Cupo is with AT&T Bell Laboratories, Middletown, NJ 07748.
R. D. Gitlin is with AT&T Bell Laboratories, Holmdel, NJ 07733.
IEEE Log Number 8928317.

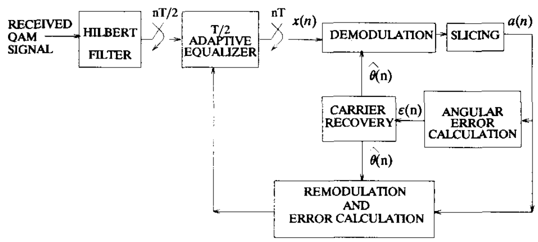

Fig. 1. Basic QAM receiver block diagram.

ω_j the frequency of the jitter and
θ_0 is the constant phase offset.

The next three sections of the text will discuss methods of compensation for $\theta(n)$.

II. The Decision-Directed Phase Locked Loop (PLL)

The first compensator to be discussed is the non-adaptive data-directed PLL [1] commonly used in QAM receivers. The loop error signal is determined by using the conjugate of the data symbol $a^*(n)$ to form

$$\operatorname{Im}\left[\frac{x(n)a^*(n)}{|a(n)|^2}\, e^{-j(\omega_c nT+\hat{\theta}(n))}\right] = \epsilon(n) \tag{3}$$

where Im denotes the imaginary part of its argument. The error signal $\epsilon(n)$ has a deterministic portion, $\sin(\theta(n) - \hat{\theta}(n))$, which for small errors is proportional to the phase error $\theta(n) - \hat{\theta}(n)$ and a random portion $\mu(n)$ which is given by $\operatorname{Im}[v(n)a^*(n)/|a(n)|^2 e^{-j(\omega_c nT+\hat{\theta}(n))}]$. Falconer [1] originally proposed a first-order PLL, but we consider a PLL where the error signal is filtered by the fixed second-order IIR filter structure shown in Fig. 2. The transfer function of the loop filter is

$$H_P = \frac{\gamma(1-\rho z^{-1})}{(1-z^{-1})^2}. \tag{4}$$

To obtain the equivalent linear model shown in Fig. 2(b), we follow Falconer [1] and assume that $\mu(n)$ is a Gaussian noise process. With this assumption, using superposition, the closed loop transfer function can be expressed as

$$H_{\text{PLL}}(z) = \frac{\hat{\theta}(z)}{\theta(z)} = \frac{H_P(z)}{1+z^{-1}H_P(z)} = \frac{\gamma(1-\rho z^{-1})}{1-(2-\gamma)z^{-1}+(1-\gamma\rho)z^{-2}} \tag{5}$$

where $\theta(z)$ and $\hat{\theta}(z)$ are the Z transforms of $\theta(n)$ and $\hat{\theta}(n)$, respectively.

Fig. 3 shows several plots of the magnitude of H_{PLL} using different values for the parameter ρ, selecting a fixed gain coefficient γ for a symbol rate of 2400 baud. From Fig. 3, one can see that the PLL is a nonadaptive, low-pass filter, whose bandwidth must be selected by the designer. Generally, the PLL parameters are chosen and fixed to achieve a compromise between a wide-band system for the purpose of tracking the phase jitter and a narrow-band system to minimize the noise enhancement.

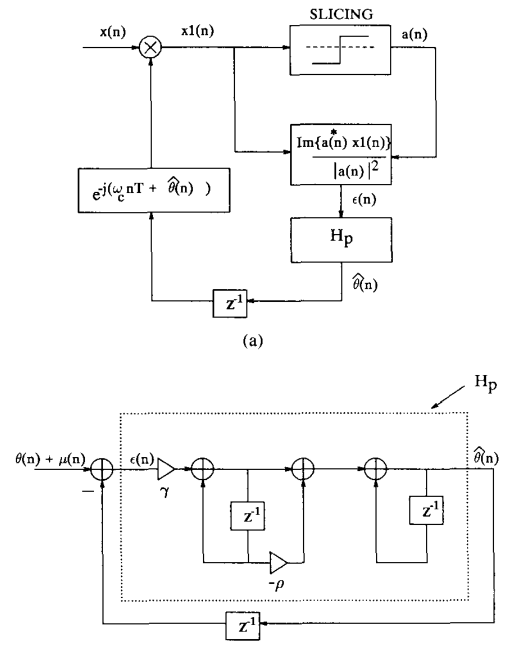

Fig. 2. Carrier recovery system using phase locked loop (PLL). (a) Block diagram with receiver. (b) Equivalent linear model of the system shown in (a).

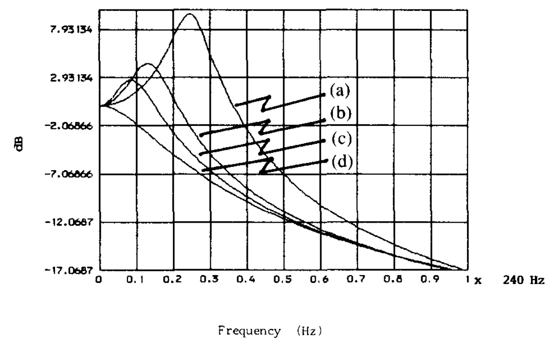

Fig. 3. PLL magnitude response for $\gamma = 0.080625$ and: (a) $\rho = 0.7$, (b) $\rho = 0.9$, (c) $\rho = 0.95$, (d) $\rho = 0.99976$.

To verify that the PLL can correct for impairments of frequency offset and phase offset, we shall make use of the final value theorem,

$$\lim_{n\to\infty} \epsilon(n) = \lim_{z^{-1}\to 1} (1-z^{-1})E(z), \tag{6}$$

where $\epsilon(n)$ is the PLL's angular error estimate and $E(z)$ is its Z transform. Let us begin by examining phase offset. For this case,

$$\theta(z) = \frac{\theta_0}{1-z^{-1}} \tag{7}$$

and referring to Fig. 2,

$$E(z) = \frac{1}{1 + H_p(z)z^{-1}}\,\theta(z). \tag{8}$$

Using the second-order PLL given in (4) results in

$$\lim_{n\to\infty} \epsilon(n) = \lim_{z^{-1}\to 1}\left[\frac{\theta_0(1 - z^{-1})(1 - z^{-1})}{(1 - z^{-1})^2 + \gamma z^{-1}(1 - \rho z^{-1})}\right]. \tag{9}$$

Equation (9) shows that the angular error $\epsilon(n)$ becomes identically zero as $n \to \infty$ (i.e., the phase offset has been *completely* removed). For frequency offset,

$$\theta(z) = \frac{z^{-1}\omega_o T}{(1 - z^{-1})^2}, \tag{10}$$

the steady-state phase error is given by

$$\lim_{n\to\infty} \epsilon(n) = \lim_{z^{-1}\to 1}\left[\frac{z^{-1}(1 - z^{-1})\omega_o T}{(1 - z^{-1})^2 + \gamma z^{-1}(1 - \rho z^{-1})}\right]. \tag{11}$$

Once again, (11) shows that the second-order PLL will compensate completely for frequency offset.

As mentioned previously, the PLL provides a compromise between jitter compensation and noise enhancement. For a high-performance carrier recovery system, a structure is sought that will *adaptively* synthesize the jitter signal to reduce the effect of noise enhancement and which will have the capability to track jitter with multiple frequencies. Structures that achieve this objective will be the subject of the next two sections.

III. An Adaptive FIR Phase Predictor

A. Basic Structure

The first proposal for adaptive phase jitter tracking was made by Gitlin [2], and was later studied by Gooch and Reddy [3]. The essential idea behind this technique is to predict the next phase estimate based on several past phase estimates using a *f*inite *i*mpulse *r*esponse *a*daptive *l*ine *e*nhancer (FIR-ALE). In Fig. 4, the structure used in the data-directed PLL of Fig. 2, to derive the phase error of (3), is the preprocessor which provides the noisy phase error which we now denote by $\psi(n)$, to avoid confusion with $\epsilon(n)$. Thus, $\psi(n)$ is the phase error of the predictive loop, while $\epsilon(n)$ is the phase error of the PLL. Ideally, a predictor would use prior carrier phase values to produce an estimate of the next phase angle. So far, we only have access to the phase error, $\psi(n) = \theta(n) - \hat{\theta}(n) + \mu(n)$. However, by adding $\hat{\theta}(n)$ to $\psi(n)$, we obtain $\theta(n) + \mu(n)$, a *noisy* estimate of the phase. This quantity will serve as the input to the predictor. With this approach, the predictor H_F generates the phase estimate $\hat{\theta}(n)$ as follows:

$$\hat{\theta}(n) = \sum_{k=0}^{L-1} \alpha(k)\phi(n - k - 1) = \boldsymbol{\alpha}^T\boldsymbol{\Phi} \tag{12}$$

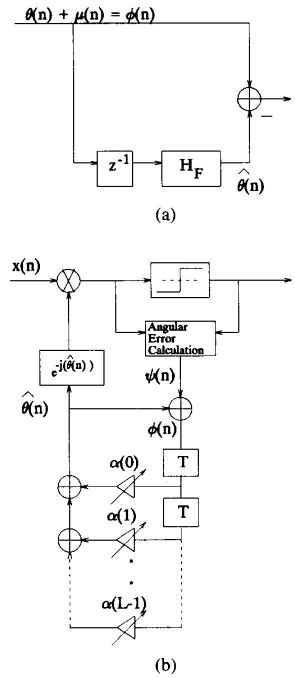

Fig. 4. FIR-ALE structure. (a) General structure. (b) Detailed structure.

where the superscript T denotes the transposed vector. The predictor has L weights

$$\boldsymbol{\alpha}^T = [\alpha_0, \alpha_1, \cdots, \alpha_{L-1}]$$

and the inputs

$$\boldsymbol{\Phi}_T = [\phi(n - 1), \phi(n - 2), \cdots, \phi(n - L)],$$

and where we have the defining relationships

$$\phi(n) = \hat{\theta}(n) + \psi(n) = \theta(n) + \mu(n),$$

for the noisy estimate of $\theta(n)$.

With the above formulation, the phase estimate is a linear combination of prior phases. Consequently, a unimodal performance surface may be formed. The optimum set of tap weights can be determined adaptively via the LMS algorithm. The performance measure we adopt is the observable mean-squared phase error,

$$J = \langle \psi(n)^2 \rangle. \tag{13}$$

Expanding J, using (12) and taking expectations gives

$$\begin{aligned} J = &\sum_{k=0}^{L-1}\sum_{k'=0}^{L-1} \alpha(k)\alpha(k')\left[r_{\theta\theta}(k - k') + \delta(k - k')\sigma_\mu^2\right] \\ &- 2\sum_{k=0}^{L-1} \alpha(k)\left[r_{\theta\theta}(k - 1) + \delta(k - 1)\sigma_\mu^2\right] \\ &+ \sigma_\mu^2 + r_{\theta\theta}(0) \end{aligned} \tag{14}$$

where $\delta(m)$ is the Kronecker delta function, σ_μ^2 is the variance of the noise component $\mu(n)$, and $r_{\theta\theta}(k)$ is the autocorrelation function of $\theta(n)$. Equation (14) has been derived assuming that the noise component $\mu(n)$ is zero mean white and uncorrelated with the jitter component $\theta(n)$. Differentiating (14) with respect to $\boldsymbol{\alpha}$, and setting the result equal to zero gives the Wiener solution for the tap weights:

$$\boldsymbol{\alpha}_{\text{opt}} = \boldsymbol{R}^{-1}\boldsymbol{p} \tag{15}$$

where

$$\boldsymbol{R} = E[\boldsymbol{\Phi}(n)\boldsymbol{\Phi}(n)^T]$$
$$\boldsymbol{p} = E[\phi(n)\boldsymbol{\Phi}(n)].$$

Thus, there exists a *unique* optimum set of parameters, $\boldsymbol{\alpha}_{\text{opt}}$. The LMS algorithm [4] may be used to adapt the alpha parameters via

$$\boldsymbol{\alpha}(n+1) = \boldsymbol{\alpha}(n) + \Delta\psi(n)\boldsymbol{\Phi}(n) \tag{16}$$

where Δ is the step size of the adaptive algorithm.

B. The FIR Step Size

To determine the range of step sizes so that (16) converges we follow the standard analysis [4] for the evaluation of the error in the filter tap weights. Let

$$\boldsymbol{V}(k) \triangleq \boldsymbol{\alpha}_{\text{opt}} - \boldsymbol{\alpha}(k) \tag{17}$$

denote the tap weight error. Using (15), (16), and (17), the tap weight error is governed by

$$\boldsymbol{V}(k+1) = [\boldsymbol{I} - \Delta\boldsymbol{R}]\boldsymbol{V}(k). \tag{18}$$

Making use of a similarity transformation, as in [4], the optimal Δ is

$$0 < \Delta < 2/\lambda_{\max} \tag{19}$$

where $\lambda_{\max}$ is the maximum eigenvalue which must be smaller than the trace of the R matrix. For the case of sinusoidal jitter with a uniformly distributed random phase ρ_m, it can be shown that

$$0 < \Delta < \frac{2}{L\left[\sum_{m=0}^{J}\frac{A_m^2}{2} + \sigma_\mu^2\right]}. \tag{20}$$

C. Compensation Ability of the FIR-ALE in the Presence of Phase Jitter

We calculate the optimal solution, $\boldsymbol{\alpha}_{\text{opt}}$, due to the superposition of the phase jitter and noise. First consider the elements of the autocorrelation matrix of a single sinusoid in noise,

$$\begin{aligned} r_{\phi\phi}(n-m) &= \frac{A_0^2}{2}[\cos\omega_0 nT\cos\omega_0 mT + \sin\omega_0 nT\sin\omega_0 mT] \\ &\quad + \sigma_\mu^2\delta(n-m). \end{aligned} \tag{21}$$

The matrix $\boldsymbol{R}$, which is comprised of elements $r_{\phi\phi}$, can be written as

$$\boldsymbol{R} = \frac{A_0^2}{2}[\boldsymbol{g}\boldsymbol{g}^T + \boldsymbol{h}\boldsymbol{h}^T] + \sigma_\mu^2\boldsymbol{I} \tag{22}$$

where $\boldsymbol{g}$ and $\boldsymbol{h}$ have elements

$$g_m = \cos\omega_0 mT$$
$$m = 0, 1, \cdots, L-1$$
$$h_m = \sin\omega_0 mT.$$

In the form expressed by (22), R is the sum of an identity matrix and two dyads $\boldsymbol{g}\boldsymbol{g}^T$ and $\boldsymbol{h}\boldsymbol{h}^T$. Using this notation the Wiener equations of (15) become:

$$\left[\frac{A_0^2}{2}(\boldsymbol{g}\boldsymbol{g}^T + \boldsymbol{h}\boldsymbol{h}^T) + \sigma_\mu^2\boldsymbol{I}\right]\boldsymbol{\alpha} = \frac{A_0^2}{2}\boldsymbol{g}. \tag{23}$$

If the filter length L is chosen such that exactly one-half the period of the unknown jitter frequency is spanned, i.e.,

$$L = \frac{k\pi}{\omega_0 T} \qquad k = 1, 2, \cdots \tag{24}$$

some interesting results and insights can be obtained. First, the following orthogonality conditions will exist

$$\boldsymbol{g}^T\boldsymbol{h} = \sum_{j=0}^{L-1}\cos\omega_0 jT\sin\omega_0 jT = \frac{1}{2}\sum_{j=0}^{L-1}\sin\frac{2jk\pi}{L} = 0 \tag{25}$$

and

$$\begin{aligned} \boldsymbol{g}^T\boldsymbol{g} &= \sum_{m=0}^{L-1}\cos^2\omega_0 mT = \frac{L}{2} + \sum_{m=0}^{L-1}\cos\frac{2\pi km}{L} \\ &= \frac{L}{2} = \boldsymbol{h}^T\boldsymbol{h}. \end{aligned} \tag{26}$$

Second, to determine the optimal vector $\boldsymbol{\alpha}_{\text{opt}}$ we make use of the identity

$$[\boldsymbol{I} + \lambda(\boldsymbol{g}\boldsymbol{g}^T + \boldsymbol{h}\boldsymbol{h}^T)]^{-1} = \boldsymbol{I} - \frac{\lambda(\boldsymbol{g}\boldsymbol{g}^T)}{1 + \lambda\boldsymbol{g}^T\boldsymbol{g}} - \frac{\lambda\boldsymbol{h}\boldsymbol{h}^T}{1 + \lambda\boldsymbol{h}^T\boldsymbol{h}}. \tag{27}$$

After some manipulation, the optimum weight vector can be shown to be

$$\boldsymbol{\alpha}_{\text{opt}} = \left[\frac{1}{\frac{2\sigma_\mu^2}{A_0^2} + \frac{L}{2}}\right]\boldsymbol{g}. \tag{28}$$

Equation (28) shows that since R is corrupted by noise, the level of the noise power will affect the optimal solution, and that for sinusoidal phase jitter, the optimal coefficients are themselves samples of a sinusoid of frequency ω_0, the jitter frequency. Note from (28) that if the jitter vanishes, $\boldsymbol{\alpha}_{\text{opt}}$ will become zero and noise enhancement will *not* occur. This is in sharp contrast to the conventional PLL.

Applying the final value theorem to the observable angular error as in (6), for the case of noiseless sinusoidal phase jitter using the structure of Fig. 4, results in

$$\lim_{n \to \infty} \psi(n) = \lim_{z^{-1} \to 1} (1 - z^{-1}) \cdot \frac{(1 - H_F(z)z^{-1})A_0 \sin \omega_0 T z^{-1}}{1 - 2 \cos \omega_0 T z^{-1} + z^{-2}} \tag{29}$$

where $H_F(z)$ is the transfer function of the FIR-ALE, i.e., $H_F(z) = \alpha_0 + \alpha_1 z^{-1} + \alpha_2 z^{-2} + \cdots + \alpha_{L-1} z^{-(L-1)}$. Equation (29) shows that $\psi(\infty)$ is indeed equal to zero.

D. Compensation Ability of the FIR-ALE in the Presence of Phase Offset

In order for an optimal (Wiener) solution to exist as in (15), the autocorrelation matrix R must be of full rank. For the case of phase offset, in the absence of noise,

$$r_{\theta\theta}(k) = \theta^2 \text{ for all } k. \tag{30}$$

Thus, under these circumstances, the FIR-ALE will not be able to track a phase offset. This is not a serious problem since passband equalizers [5] are able to compensate for phase offset.

Using the final value theorem,

$$\lim_{n \to \infty} \psi(n) = \lim_{z^{-1} \to 1} \theta_0 [1 - H_F(z) z^{-1}]. \tag{31}$$

If $H_F(1) = 1$, the FIR-ALE could compensate for phase offset, but as we show in the next section, the FIR-ALE has difficulty with frequency offset and a separate subsystem will be needed to compensate for these impairments.

E. Compensation Ability of the FIR-ALE in the Presence of Frequency Offset

An optimal solution does not exist for frequency offset. Moveover, the FIR filter is rendered unstable in the presence of frequency offset. This can be seen by evaluating the non-stationary autocorrelation function as

$$r_{\theta\theta}(k; n) = (\omega_o T)^2 n(n + k), \tag{32}$$

which is clearly unbounded for increasing n. Furthermore, the final value theorem states that

$$\lim_{n \to \infty} \psi(n) = \lim_{z^{-1} \to 1} \left[\frac{\omega_o T}{1 - z^{-1}} \right] z^{-1} [1 - H_F(z) z^{-1}]. \tag{33}$$

Only for the case when $H_F(z) = 1$, ($\alpha_0 = 1$, $\alpha_i = 0$ $i \neq 0$) is compensation possible as $\psi(\infty)$ is finite. Actually, $H_F(z) = 1$ implements a simple first order PLL which can compensate for frequency offset following reasoning similar to (11). This suggests preceding the FIR filter with a second-order PLL for complete frequency and phase offset compensation. With these observations, we shall use the structure of Fig. 5, with a very narrowband PLL, to implement our carrier recovery system.

F. The Need for Leakage

The bias inherent to most digital implementations causes the effect of coefficient drifting as seen in fractionally spaced equalizers [6]. This has been noticed experimentally for the FIR-ALE. A small leakage [6], μ, equal to 1/2 the LSB of the tap coefficients was used and the system was stabilized. Using leakage, the update equation (16) becomes

$$\boldsymbol{\alpha}(n + 1) = (1 - \mu)\boldsymbol{\alpha}(n) + \Delta\psi(n)\boldsymbol{\Phi}(n). \tag{34}$$

Applying the same type of analysis as in Section III, the step size is bounded by

$$\frac{-\mu}{L\left[\sum_{m=0}^{J} \frac{A_m^2}{2} + \sigma_\mu^2\right]} < \Delta < \frac{\mu + 1}{L\left[\sum_{m=0}^{J} \frac{A_m^2}{2} + \sigma_\mu^2\right]}. \tag{35}$$

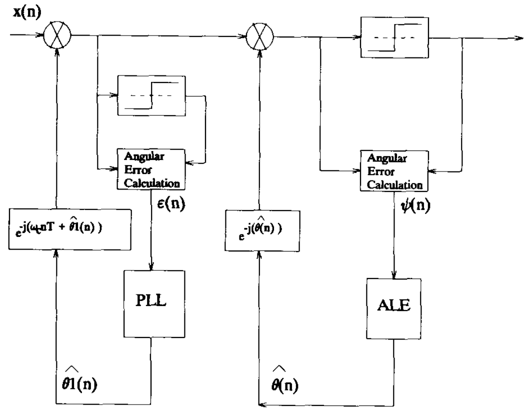

Fig. 5. Carrier recovery structure used to compensate for frequency/phase offset and phase jitter. The narrowband PLL on the left compensates for frequency and phase offset, and the ALE tracks jitter.

G. Selecting the Filter Length

To select the parameter L, from (24), a sufficient condition for detection is to span 1/2 the period of the incoming sinusoid. However, it appears (24) provides an upper bound on the requirements of L. Shorter lengths may suffice at a possible cost of less attenuation of the incoming jitter. Theoretically speaking, as L increases towards infinity without any background noise, the error in (13) approaches zero. However, practically speaking, an increase in L increases the misadjustment of the process [4]. Also, there is a point of diminishing returns in performance. This point is seen somewhere between 20 to 30 taps for 60 Hz jitter. At a baud of 2400, 20 taps will span one-half of the period of a 60 Hz sinusoid. To compensate for lower frequencies, say 20 Hz, this requirement becomes 60 taps. The use of sparse taps, i.e., spacing greater than T, could then be applied. That is, use 30 taps and $2T$ spacing, to compensate for 20 Hz jitter. The sparse taps simply change the effective baud.

IV. An Adaptive IIR Phase Predictor

A. Basic Structure

A second option for phase prediction utilizes an IIR filter structure for jitter compensation. We start with the structure of Fig. 5 where the ALE portion is now replaced by an IIR-ALE. There are two well-known problems with adaptive IIR filters: 1) the possibility of the filter becoming unstable during adaptation and 2) the existence of local minima. With these problems in mind, our approach to the IIR-ALE centers around the implementation of an adaptive notch filter by placing complex conjugate poles close to the unit circle on a *fixed* radius. The angular placement of the poles around the unit circle will be varied. This corresponds to altering the location, in frequency, of the resonance of the filter structure. More specifically, we choose a model transfer function as in [7]–[10] with the modification that due to finite precision effects, our implementational vehicle will be a 2 multiplier lattice filter [11], [12] as shown in Fig. 6. This structure is based on orthogonal polynomials and typically possesses better quantization properties than those structures based on direct-form canonic realizations [11]. The filter input is $\phi(n-1)$ as in (12).

The transfer function between $\hat{\theta}(n)$ and $\phi(n)$ in our model, which can handle the tracking of a single sinusoid can be written as

$$H_I(z) = \frac{-k_0 z^{-1} - z^{-2}}{1 + k_0(1 + r^2)z^{-1} + r^2 z^{-2}}. \tag{36}$$

As such, the reflection and tap parameters can be written as

$$k_1 = r^2 \tag{37a}$$

$$k_0 = \hat{k}_0(n) \tag{37b}$$

$$V_2 = -1.0 \tag{37c}$$

$$V_1 = r^2 \cdot k_0 \tag{37d}$$

$$V_0 = r^2 - k_0 \cdot V_1 \tag{37e}$$

where k_0 will be adjusted to select the center frequency of the filter and r is a filter parameter which is representative of the fixed pole radius. The nodal equations of the two multiplier lattice structure of Fig. 6 are

$$a_1(n) = \phi(n-1) - r^2 b_1(n-1) \tag{38a}$$

$$b_0(n) = a_1(n) - k_0(n) b_0(n-1) \tag{38b}$$

$$b_1(n) = k_0(n) b_0(n) + b_0(n-1) \tag{38c}$$

$$b_2(n) = r^2 a_1(n) + b_1(n-1) \tag{38d}$$

and the phase estimate is

$$\hat{\theta}(n) = \sum_{i=0}^{2} V_i b_i(n). \tag{38e}$$

To correct for more than one frequency, a multiple-section transfer function will be needed. Section IV-D addresses this issue.

The actual complex-conjugate pole locations can be found by computing the roots of the denominator polynomial of (36). Defining the position of the poles in the z-plane as $z_{1,2} = r' e^{\pm j\omega_0' T}$, we wish to determine the pole radius r' and the angular placement of the poles $\omega_0' T$ in terms of the filter parameters r and k_0. The pole locations are

$$r'^2 = \cos^2 \omega_0 T \frac{(1 + r^4)}{2} + r^2 \sin^2 \omega_0 T$$
$$\omega_0' T = \tan^{-1}\left[\frac{4r^2 \sec^2 \omega_0 T}{(1 + r^2)^2} - 1\right]^{1/2}. \tag{39}$$

It can be seen that as the filter parameter r approaches unity, the pole radius r' approaches unity and the angular displacement of the poles $\omega_0' T$ becomes $\omega_0 T$, the frequency of the unknown sinusoid. Thus, we shall strive to make r very close to unity.

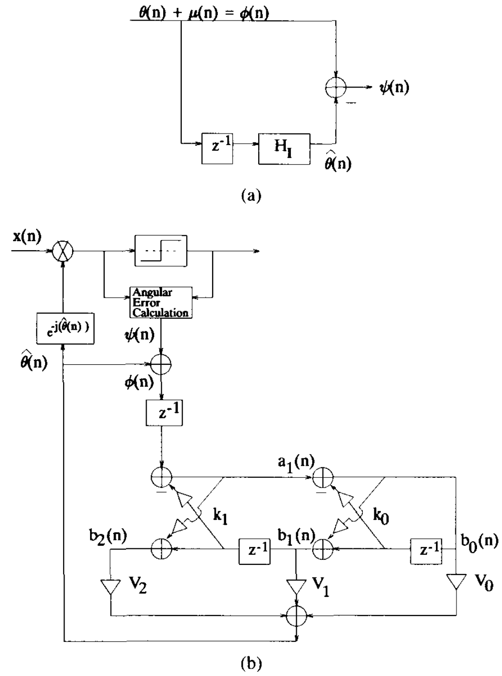

Fig. 6. IIR-ALE structure. (a) General structure. (b) Two multiplier lattice form of IIR-ALE.

B. The IIR Optimal Solution

The Z-transform of the error $\psi(n)$ of the IIR-ALE System to be minimized can be written as

$$\psi(z) = \left(1 - z^{-1} H_I(z)\right)\theta(z), \tag{40}$$

and the mean-squared phase error, for a single sinusoid in white noise is given by

$$\begin{aligned}\langle \psi^2(n) \rangle &= \int \psi(z)\psi^*(z) z^{-1}\, dz \\ &= \frac{A_0^2}{2}\left|1 - e^{-j\omega_0 T} H_I(e^{j\omega_0 T})\right|^2 + 2\sigma_\mu^2/(1 + r^2).\end{aligned} \tag{41}$$

The optimal solution can be found by substituting (36) into (41) and setting the derivative of (41) with respect to

k_0 to zero resulting in a *unique* value of k_0 that minimizes (41):

$$k_0^* = -\cos \omega_0 T. \tag{42}$$

C. Performance Surface of the IIR Predictor

As mentioned in Section III, a major advantage of an FIR-ALE is the fact that the error surface is unimodal and quadratic. In this section, we shall examine the performance surface of the IIR predictor to determine under what conditions it is unimodal. We shall begin by examining (41). The adaptive parameter k_0, will be plotted for various *fixed* values of r given a certain input jitter frequency ω_0. Fig. 7 shows the normalized (with respect to input jitter power) case where ω_0 corresponds to 300 Hz with 20 dB SNR (A_0^2 relative to σ_μ^2). Here, r^2 is varied from 0.9625 (bandwidth = 19 Hz, given 2743 symbols/s) to 0.6625 (bandwidth = 182 Hz, given 2743 symbols/s) with integer coefficients, as would be used in a Digital Signal Processor (DSP) chip. Note that Fig. 7 shows two scales for its x-axis. The first scale represents the value of k_0 as it is varied from -1 to approximately -0.5. The second scale printed directly below the first corresponds to the frequency determined by the specific value of k_0 from the first scale as calculated from (42). Notice that although the error surface is indeed *unimodal*, the surface flattens away from the minimum, as the poles approach the unit circle. Furthermore, although not shown here, as the frequency of the input sinusoid ω_0 increases, the surface flattens out even for smaller radii. These facts were also noted in [7]–[10], where instead of a pure gradient search technique, a normalized form was applied, where the normalization is used to speed convergence when the gradient is small. While well suited to a main frame computer with nearly infinite precision floating point representation, a signal processing chip affords much less computational power and precision. As such, we seek a successful search using the LMS [4] algorithm.

D. Multiple Sinusoids

As a second-order section can compensate for only one frequency, we shall now turn our attention to the signal environment possessing multiple sinusoidal frequencies. To derive the performance surface, we observe that when the input jitter consists of J tones we have that

$$\Phi_{\phi\phi}(e^{j\omega T}) = \sum_{j=0}^{J} \frac{A_j}{4}\left[\delta(\omega T - \omega_j T) + \delta(\omega T + \omega_j T)\right] + \sigma_\mu^2, \tag{43}$$

and (41) becomes

$$\langle \psi(n)^2 \rangle = \sum_{j=0}^{J} \frac{A_j^2}{2}\left|1 - e^{-j\omega_j T} H_{I_j}(e^{j\omega_j T})\right|^2 + 2\sigma_\mu^2/(1 + r^2) \tag{44}$$

where H_{I_j} is one of $(J + 1)$ transfer functions of the form given in (36).

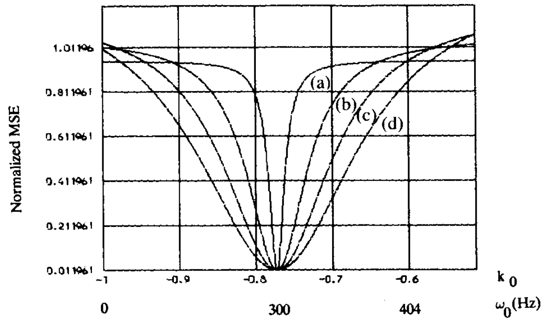

Fig. 7. IIR-ALE performance surface for $\omega_0 = 300$ Hz and 20 dB SNR: (a) $r^2 = 0.9625$, (b) $r^2 = 0.8625$, (c) $r^2 = 0.7625$, (d) $r^2 = 0.6625$.

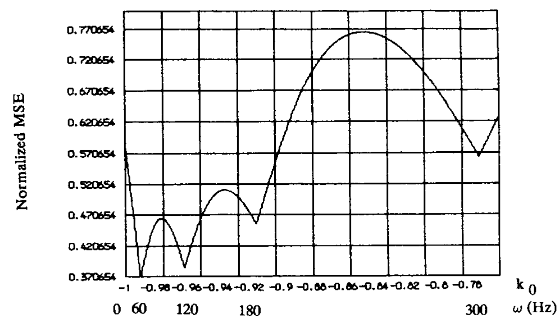

Fig. 8. IIR-ALE performance surface for 20 dB SNR and: (a) $A0 = A1 = A2 = A3$. (b) $\omega_0 = 60$ Hz, $\omega_1 = 120$ Hz, $\omega_2 = 180$ Hz, $\omega_3 = 300$ Hz. (c) $r^2 = 0.7625$.

Fig. 8 presents the surface for the case where 1) $J = 3$, 2) $A_0 = A_1 = A_2 = A_3$, and 3) $\omega_0 = 60$ Hz, $\omega_1 = 120$ Hz, $\omega_2 = 180$ Hz, and $\omega_3 = 300$ Hz. Note that there are four local minima in the surface, corresponding to the various locations of ω_j. With multiple jitter frequencies present at the input, the performance surface is indeed multimodal relative to the IIR adjustable parameters; however, by sequential adjustment of the filter, we can optimize the overall filter structure. That is, we desire to identify each and every local minima. The hypothesis made here is that if the algorithm of Section IV-E is applied one section at a time, that section will remove the strongest tone leaving the others unaltered. Other sections can be added one-by-one until all that is left in the spectrum is noise. Each section is capable of attenuating any tone to a level at which it is not detectable by the next section, thereby removing one null from the performance surface. When all tones have been removed, the performance surface due to noise will be flat such that when starting another section, the gradient will be zero and that section will not move away from its initial 0 Hz starting point.

Using this procedure, we have handled the condition of under and over-modeling. For undermodeling (number of sections < number of sinusoids) because of the narrowband structure of the predictor, as many sinusoids are removed as sections exist. Overmodeling is handled by observing when the last section remains at 0 Hz. To compensate for two frequencies, the structure of Fig. 9 will be used.

E. Adaptive Algorithm for the IIR-ALE

We shall begin by assuming the input error has only a single sinusoid. As such, only one IIR section is required. After studying the surfaces expected in this application, one can conclude that a radius of $r^2 = 0.76$ is adequate to guarantee convergence of the LMS algorithm for frequencies up to 300 Hz, the highest phase jitter frequency for our application. This radius provides adequate slope to the gradient and has a *single minimum* corresponding to the frequency of the single sinusoid. As done in (13) for the FIR-ALE, the mean square error of $\psi(n)$ will be minimized. Recall that we only adapt one parameter k_0 per second-order section. As such, the LMS update becomes

$$k_0(n) = k_0(n-1) + \eta\psi(n)\theta_k(n) \quad n = 1, 2, 3, \cdots \tag{45}$$

where

η is the step size of the algorithm

$$\theta_k(n) = \frac{\partial\hat{\theta}(n)}{\partial k_0} = \frac{-\partial\psi(n)}{\partial k_0}.$$

To calculate the total gradient $\theta_k(n)$ we compute $\partial\hat{\theta}(n)/\partial k_o$ using the following relations and (38):

$$\alpha_1(n) = \frac{\partial a_1(n)}{\partial k_0} = -r^2\beta_1(n-1) \tag{46a}$$

$$\beta_0(n) = \frac{\partial b_0(n)}{\partial k_0} = \alpha_1(n) - b_0(n-1) - k_0(n)\beta_0(n-1) \tag{46b}$$

$$\beta_1(n) = \frac{\partial b_1(n)}{\partial k_0} = b_0(n) + k_0(n)\beta_0(n) + \beta_0(n-1) \tag{46c}$$

$$\beta_2(n) = \frac{\partial b_2(n)}{\partial k_0} = r^2\alpha_1(n) + \beta_1(n-1), \tag{46d}$$

which finally gives

$$\theta_k = \frac{\partial\hat{\theta}(n)}{\partial k_0} = \left[\sum_{i=0}^{2} V_i\beta_i(n)\right] + r^2 b_1(n) - 2r^2 k_0(n) b_0(n). \tag{46e}$$

Once the equations in (46) are computed and k_0 updated via (45), $V_1(n)$ and $V_2(n)$ can be computed via (37).

A short discussion on the selection of r^2 is in order at this point. First, from the performance surface section, smaller values of r^2 (large bandwidth) allow for greater concavity of the performance surfaces. However, as r^2 approaches unity greater reduction in angular error arises. Thus, one may desire to shift gears between a radius which allows for k_0 to converge close to optimum and another larger radius which fine tunes the estimate and reduces energy in $\psi(n)$. This is the approach taken in the experimental results reported in Section VI.

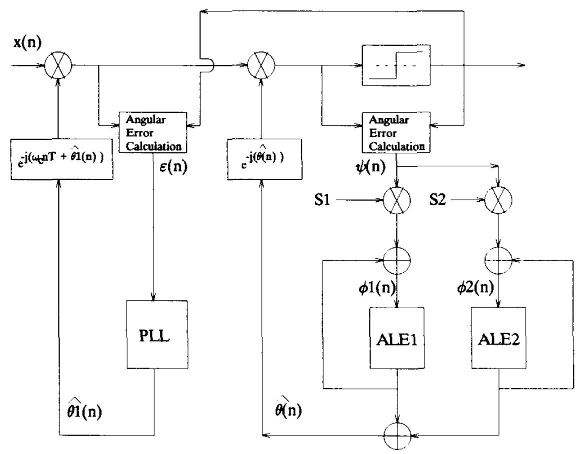

Fig. 9. Two section IIR-ALE carrier recovery system for tracking multiple jitter frequencies.

F. Final Value Theorem Results on the IIR-ALE

As done for Section III, we shall apply the final value theorem to the single section IIR-ALE. Inasmuch as the IIR-ALE is solely used to compensate for phase jitter, we shall precede it by a second-order PLL to compensate for phase offset and frequency offset. Thus, we shall only consider the IIR-ALE's response to sinusoidal jitter. To do this we consider

$$\lim_{n\to\infty}\psi(n) = \lim_{z^{-1}\to 1}(1 - z^{-1})\left(\frac{2 + r^2}{1 + r^2}\right) \cdot \frac{A_0 \sin \omega_0 T z^{-1}}{1 - 2\cos\omega_0 T z^{-1} + z^{-2}} = 0. \tag{47}$$

Thus, phase jitter of a single tone can be completely compensated for within a single section IIR-ALE.

V. Structure Comparisons

The previous two sections discussed various attributes of FIR and IIR-ALE's. This section will contrast the two approaches with respect to system parameters. A 19.2 Kbit/s system using 7 bits/symbol and 2743 symbols/s will be utilized for real time results.

A. Filter Length

The IIR-ALE under discussion has only one adaptive parameter per sinusoid. The resolution (minimum detectable frequency) of the predictor is determined by the larger of a) the number of bits used to represent k_0 and b) the radius of the model. Given a 16 bit k_0, the smallest nonzero angle representable in the current implementation, from (42), is $\cos^{-1}(1 - 2^{-14})$. This corresponds to 5 Hz using a symbol rate of 2743. However, the theoretical resolution for the radius used within this study is somewhat greater and becomes the limiting factor in this model. To determine the resolution, consider that stability of H_I requires

$$\left|(1 + r^2)k_0\right| < 2r. \tag{48}$$

Combining (48) and (42), we note that the resolution is given by

$$\hat{\omega}_{\min} = \cos^{-1}\left(\frac{2r}{1 + r^2}\right). \tag{49}$$

Choosing $r^2 = 0.76$ results in a resolution of 59 Hz while an $r^2 = 0.96$ results in a resolution of 9 Hz. For the FIR case, using (24) to define the upper bound requirements on L, resolving a 59 Hz jitter stipulates a span of 24 symbols while 9 Hz specifies a span of 152 symbols.[1]

B. Complexity

The complexity of the IIR-ALE is considerably less than that of the FIR-ALE. This is due, in part, to the fact that the IIR-ALE updates only one tap per sinusoid. Using a DSP chip implementation vehicle, a two section IIR-ALE uses 50 percent less RAM, equivalent processing time and equivalent ROM space when compared to a 30 tap FIR-ALE. In neither implementation have we attempted to optimize any of these parameters through clever DSP coding strategies. Also, if only one IIR-ALE section is desired, the RAM and cycle times can be halved.

C. Phase Jitter Cancellation Ability

As the IIR-ALE synthesizes a deep notch, it is expected to outperform the FIR-ALE with respect to its cancellation ability. Fig. 10 shows a spectral analyzer plot of the angular error for 5° of jitter at 120 Hz before and after prediction for the case of a) IIR-ALE and b) FIR-ALE. Note that the IIR-ALE cancels 20 dB of the angular error whereas the FIR-ALE is only able to cancel 7 dB of the angular error. Thus, for these implementations, the FIR-ALE reduces 5° of jitter to 2.2° while the IIR-ALE reduces 5° of jitter to a residual value of 0.5°. The effect that this has on block error rate (BLER) will be examined in a later section.

D. Multiple Sinusoids

This section presents experimental results for the case where more than one sinusoid is present at the receiver input. In these experiments, two IIR-ALE sections will be used. Fig. 11 shows the case where two sinusoids are present. The 120 Hz tone possesses 10° of phase jitter while the 60 Hz tone had 5°. Fig. 11(a) shows that the first IIR-ALE section removed the dominant 120 Hz tone with 19 dB of cancellation. The second IIR-ALE section attenuates the 60 Hz tone also by 19 dB, as shown in Fig. 11(b). The second section is not allowed to train until the first section has converged and switched to the larger radius. On the other hand, Fig. 11(c) shows that the FIR-

[1]This requirement is overly stringent as per the discussion of Section III.

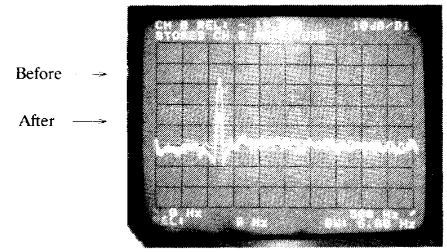

(a)

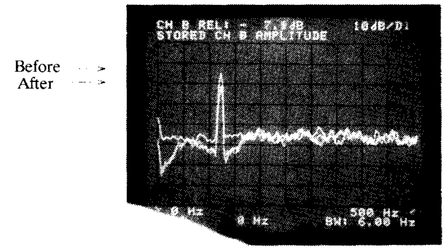

(b)

Fig. 10. Spectral analyzer plots of angular error for 5° jitter at 120 Hz before and after prediction via: (a) IIR-ALE. (b) FIR-ALE.

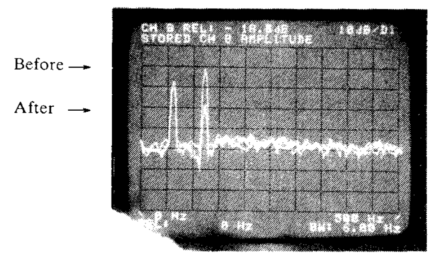

(a)

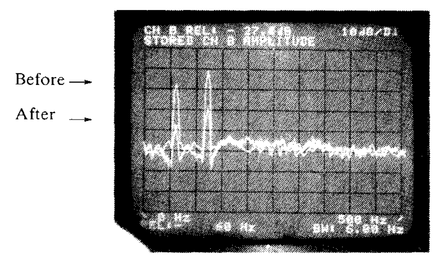

(b)

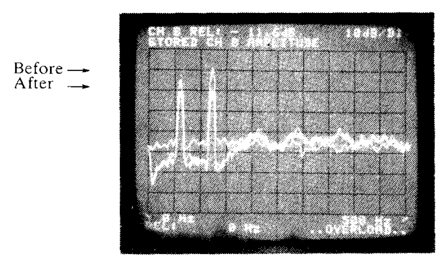

(c)

Fig. 11. Spectral analyzer plots of angular error for 5° jitter at 60 Hz and 10° jitter at 120 Hz before and after prediction via: (a) IIR-ALE Section #1. (b) IIR-ALE Sections #1 and #2. (c) FIR-ALE.

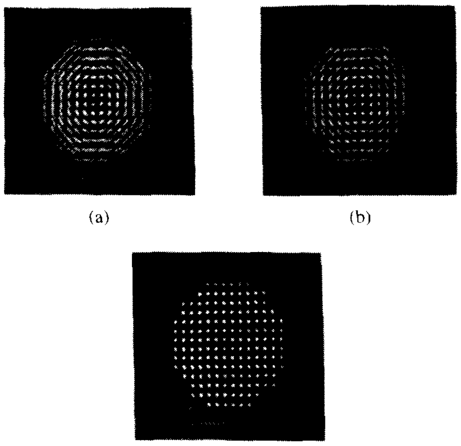

(a) (b) (c)

Fig. 12. 19.2 Kbits/s constellations for Fig. 11. (a) Before cancellation. (b) FIR-ALE. (c) Two section IIR-ALE.

ALE attenuates the 120 Hz tone by 12 dB and the 60 Hz tone by 5.8 dB. In Fig. 10, a single frequency 5° jitter was attenuated by 7 dB. Thus, although the FIR-ALE handles multiple frequencies, it does so at a cost of less attenuation per tone. Furthermore, the FIR-ALE is sensitive to the amplitude of the jitter (as evidenced by the additional 6 dB of attenuation of the 10° jitter) whereas the IIR-ALE synthesizes a 20 dB notch independent of the amount of nonzero phase jitter. This can be explained noting the absence of A_0^2 from (42) as compared to (28). Fig. 11(a) also demonstrates the condition of undermodeling. That is, given n sinusoids (2 for this case) and m IIR sections (1 for this case) m sinusoids will be tracked and $n - m$ will remain.

Finally, Fig. 12 presents 19.2 Kbits/s constellations for the environment of Fig. 11. Notice that the FIR-ALE [Fig. 12(b)] is not adequate to completely remove the visible effect of the phase jitter on the signal constellation. However, Fig. 12(c) shows that the IIR-ALE removes all visible trace of the jitter.

E. Noise Enhancement

We investigate the condition where jitter is absent and the dominant impairment is noise on a flat channel. Fig. 13 shows the results of the FIR and IIR-ALE's versus no carrier recovery loop. Both ALE's perform similarly, and are within 1/4 dB of the system that uses no carrier recovery loop at all. Thus, in the absence of jitter, forcing a carrier recovery system to adapt causes (at most) a negligible 1/4 dB loss of system performance.

F. Block Error Rate Results

Block error rate (BLER) tests were made to assess system performance improvements emanating from the additional 10 dB of cancellation afforded by the IIR-ALE. For no other impairments other than jitter and noise, BLER results are presented in Fig. 14. Fig. 14 shows that the 19.2 Kbit/s BLER of the IIR-ALE performs 3/4 dB better than the FIR-ALE for 5° of jitter and 3 dB better for 10° of jitter.

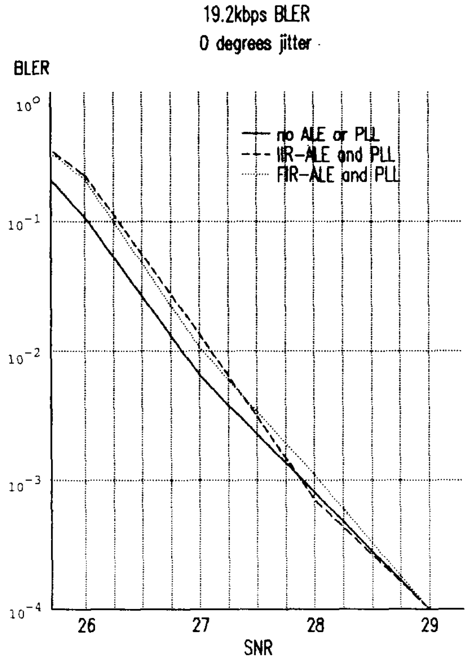

Fig. 13. Noise enhancement performance of: (a) no carrier recovery loop. (b) IIR-ALE. (c) FIR-ALE.

G. Phase Jitter Cancellation of Two Tones

Experimental results for the case of two tones of sinusoidal jitter are presented in Fig. 15. Here, 5° of jitter is applied at 100 and 120 Hz. Fig. 15 shows that a) in the absence of any carrier recovery loop, the error rate will be unity for these SNR's, b) The IIR-ALE outperforms the FIR-ALE by almost 3 dB, and c) the IIR-ALE brings performance within 0.5 dB of the case where no jitter or carrier recovery loop was present. Note that case c) above illustrates that the IIR-ALE approaches within 0.5 dB of ideal performance.

VI. Conclusions

This paper has presented and compared two novel *adaptive* carrier recovery loops for digital data communications systems with emphasis on their application to voiceband modems. The first, based on an FIR-ALE [2]–[3], offers the two major advantages of global convergence and readily handling multiple jitter frequencies. The second, based on an IIR-ALE, is computationally simple and generates a significantly greater amount of jitter cancellation than the FIR-ALE. By restricting the range of jitter frequencies to those encountered in practice, convergence of the IIR-ALE can be guaranteed. For the case of handling multiple sinusoids, the IIR-ALE requires supplying one section per expected tone. By paralleling sections, the IIR-ALE will remove a greater amount of jitter than possible with the FIR-ALE. The order selection

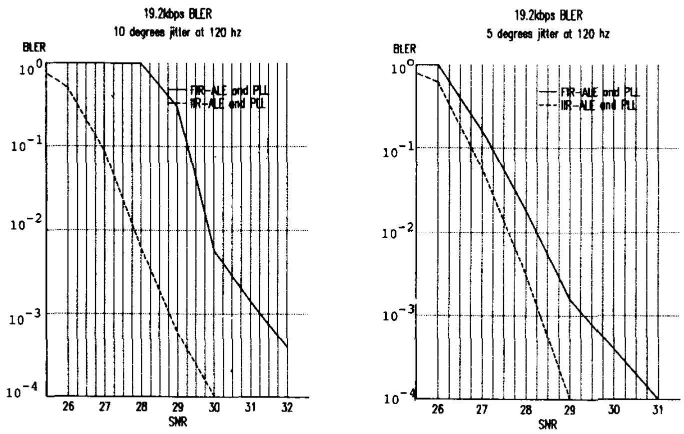

(a) (b)

Fig. 14. 19.2 Kbits/s BLER comparisons of FIR-ALE and IIR-ALE using 120 Hz jitter. (a) 10°. (b) 5°.

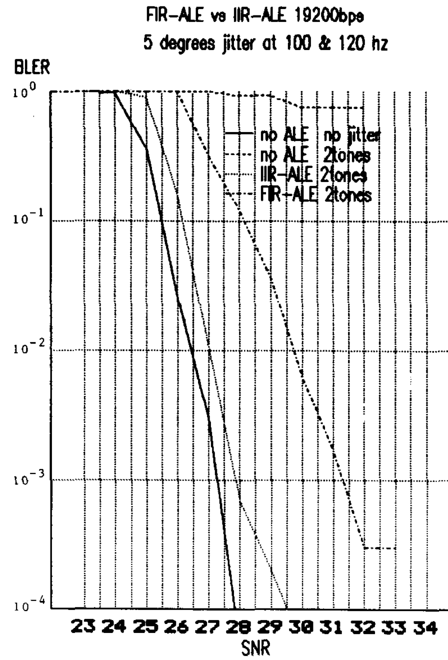

Fig. 15. 19.2 Kbits/s BLER comparisons of FIR-ALE and IIR-ALE using 5° of jitter at 120 Hz and 5° of jitter at 100 Hz.

problem (choosing correct number of sections) for the IIR-ALE is handled in the following manner. 1) Undermodeling (where the number of sinusoids exceeds the number of sections): because of the narrowband structure of the predictor, as many sinusoids are removed as sections exist. 2) Overmodeling is handled by observing when the last section remains at 0 Hz due to a flat error performance surface. Finally, the IIR-ALE provides a significant improvement in system error rate of as much as 3 dB at 19 Kbits/s, when compared to the FIR-ALE. Furthermore, given severe jitter, IIR-ALE performance can be within 0.5 dB of the ideal case where no jitter was present.

Both of the adaptive structures represent major breakthroughs in the performance attainable by carrier-recovery systems in the presence of severe jitter, in that they do not have the wide bandwidth (for tracking) versus the narrow bandwidth (for noise rejection) conflict inherent in conventional tracking loops. Consequently, these structures will provide much more reliable transmission in high-performance (>6 bits/s/Hz) digital data communications systems than conventional tracking loops. The IIR-ALE is preferable to the FIR-ALE in applications where the jitter spectrum is known *a priori* to be sinusoidal and the jitter frequencies are limited to a fraction of the symbol rate. Otherwise, the FIR-ALE, which uses no input assumptions, is preferable.

Acknowledgment

The authors are indebted to A. Montalvo for some initial work with the FIR-ALE and to R. Marabuto for providing test results. The authors also thank N. Jablon and the anonymous reviewers for their careful review of the original manuscript.

References

[1] D. D. Falconer, "Jointly adaptive equalization and carrier recovery in two-dimensional digital communication systems," *Bell Syst. Tech. J.*, vol. 55, no. 3, pp. 317–334, Mar. 1976.

[2] R. D. Gitlin, "Adaptive phase jitter tracker," U.S. Pat. 4320526, Mar. 16, 1982.

[3] R. P. Gooch and M. J. Reddy, "An adaptive phase lock loop for phase jitter tracking," *Conf. Rec., 21st Asilomar Conf. Signals, Syst., Comput.*, Nov. 2–4, 1987.

[4] B. Widrow and S. D. Stearns, *Adaptive Signal Processing*. Englewood Cliffs, NJ: Prentice-Hall, 1985.

[5] R. D. Gitlin, E. Y. Ho, and J. E. Mazo, "Passband equalization of differentially phase-modulated data signals," *Bell Syst. Tech. J.*, vol. 52, no. 2, pp. 219–238, Feb. 1973.

[6] R. D. Gitlin, H. C. Meadors, Jr., and S. B. Weinstein, "The tap-leakage algorithm: An algorithm for the stable operation of a digitally

implemented, fractionally spaced adaptive equalizer," *Bell Syst. Tech. J.*, vol. 61, no. 8, pp 1817-1839, Oct. 1982.

[7] D. R. Hush, N. Ahmed, R. David, and S. D. Stearns, "An adaptive IIR structure for sinusoidal enhancement, frequency estimation and detection," *IEEE Trans. Acoust., Speech, Signal Processing*, vol. ASSP-34, pp. 1380-1381, Dec. 1986.

[8] R. David, "Detection of multiple sinusoids using a parallel ALE," *Int. Conf. Acoust., Speech, Signal Processing*, pp. 21.2.1-21.2.4, 1984.

[9] N. Ahmed, D. Hush, G. R. Elliot, and R. J. Fogler, "Detection of multiple sinusoids using an adaptive cascaded structure," *Int. Conf. Acoust., Speech, Signal Processing*, pp. 21.3.1-21.3.4, 1984.

[10] R. A. David, S. D. Stearns, and G. R. Elliot, "IIR algorithms for adaptive line enhancement," *Int. Conf. Acoust., Speech, Signal Processing*, pp. 17-20, 1983.

[11] J. D. Markel and A. H. Gray, "Roundoff noise characteristics of a class of orthogonal polynominal structures," *IEEE Trans. Acoust., Speech, Signal Processing*, vol. ASSP-23, pp. 473-486, Oct. 1975.

[12] A. H. Gray and J. D. Markel, "A normalized digital filter structure," *IEEE Trans. Acoust., Speech, Signal Processing*, vol. ASSP-23, pp. 268-277, June 1975.

Robert L. Cupo (S'76-M'82) received the Ph.D. degree in electrical engineering from Cornell University in 1982.

Since then, he has been involved in exploratory work in high-speed modems as a Member of Technical Staff in the Data Communications Research Department at AT&T Bell Laboratories, Middletown, NJ. In February 1989, he was appointed Distinguished Member of Technical Staff. His current research interests are adaptive signal processing, spectral estimation and bandwidth efficient communications systems.

Dr. Cupo has served as a session chairman and organizer for numerous Communication Society conferences. He is also currently an Associate Editor of the IEEE COMMUNICATIONS MAGAZINE. He is a member of the Signal Processing and Communications Electronics committee of the IEEE Communications Society and Tau Beta Pi. He holds 4 patents in the area of signal processing and data communications.

Richard D. Gitlin (S'67-M'69-SM'76-F'86) was born in Brooklyn, NY, on April 25, 1943. He received the B.E.E. degree (cum laude) from the City College of New York, NY, in 1964 and the M.S. and D.Sc. degrees from Columbia University, New York, NY, in 1965 and 1969, respectively.

Since 1969, he has been with AT&T Bell Laboratories, Holmdel, NJ. From 1969 to 1979, he did applied research and exploratory development in the field of high-speed voiceband modems, with emphasis on adaptive equalization, bandwidth-efficient modulation, echo cancellation, carrier and timing recovery, and digital signal processing. From 1979 to 1982 he supervised a group doing exploratory and advanced development in these areas. From 1982 to 1987 he was head of a department responsible for systems engineering, exploratory development, and final development of data communications equipment. Currently, he is head of the Network Systems Research Department where he manages research in lightwave networks, packet switching, data networking, and broadband networking.

Dr. Gitlin is the author of more than 40 technical papers, numerous conference papers, and he holds 19 patents in the areas of data communications and digital signal processing. He is coauthor of a paper on fractionally spaced adaptive equalization that was selected as the Best Paper in Communications by the *Bell System Technical Journal* in 1982. He is a member of Sigma Xi, Tau Beta Pi, and Eta Kappa Nu. Currently, he is Chairman of the Communication Theory Committee of the IEEE Communications Society, as well as a member of the COMSOC Awards Board. Previously, he was Editor for Communication Theory of the IEEE TRANSACTIONS ON COMMUNICATIONS, and a member of the Editorial Advisory Board of the PROCEEDINGS OF THE IEEE. In 1985 he was elected a Fellow of the IEEE for his contributions to data communications technology, and in 1987 he was named an AT&T Bell Laboratories Fellow.